Solving Orientation Duality for 3D Circular Features using Monocular Vision

Alaa AlZoubi[1], Tanja K. Kleinhappel[2], Thomas W. Pike[2], Bashir Al-Diri[1] and Patrick Dickinson[1]
[1]*School of Computer Science, University of Lincoln, Lincoln, U.K.*
[2]*School of Life Sciences, University of Lincoln, Lincoln, U.K.*

Keywords: 3D Orientation, Circular Feature, Covariance Matrix, Monocular Vision.

Abstract: Methods for estimating the 3D orientation of circular features from a single image result in at least two solutions, of which only one corresponds to the actual orientation of the object. In this paper we propose two new methods for solving this "orientation duality" problem using a single image. Our first method estimates the resulting ellipse projections in 2D space for the given solutions, then matches them against the image ellipse to infer the true orientation. The second method compares solutions from two co-planar circle features with different centre points, to identify their mutual true orientation. Experimental results show the robustness and the effectiveness of our methods for solving the duality problem, and perform better than state-of-art methods.

1 INTRODUCTION

Estimating the 3D orientation of a circular feature is a common task in computer vision, with a wide range of applications in 3D pose estimation (Safaee-Rad et al., 1992), object tracking (Yoon et al., 2003), eye gaze estimation (Wang et al., 2003), camera calibration (Chen et al., 2004), and recently for GEO spacecraft pose estimation (Xu et al., 2012) and mobile robot tracking. Circular features can also provide important clues for 3D object orientation, the perspective projection in any arbitrary orientation is an exact ellipse, which can be defined with only three parameters, and can be located with high accuracy in images (Young, 1987). (Safaee-Rad et al., 1992) proposed a closed-form solution which has shown high accuracy, but which results in two solutions. Existing methods for disambiguating these solutions, and solving the duality problem, have made use a second image taken from a different relative camera position. However, such solutions are not applicable for moving objects, and require two clear images of the object, which is not always possible or convenient.

In this paper we present two novel methods for solving this duality problem which require only a single image. We describe these methods as a part of an application framework which we have developed for tracking and identifying tagged fish (supporting biological research studies in a laboratory environment). Our ultimate objective is to use the circular features in recognition of moving objects. The contributions of this paper are: (1) developing two new methods to solve the orientation duality problem for 3D circular features using a single 2D image. The first method compares features from the 2D projects of both solutions with the image ellipse in the image plane. The method has the advantages of requiring only a single image, and does not require additional geometric features or image texture, nor an estimate of the 3D position of the object. The second method uses two non-coinciding co-planar circular features, and similarly does not require multiple images, and does not require image texture, nor a position estimate. (2) we provide experimental results which show the performance of our methods on sets of images of circular objects with different diameters and orientations. A comparison with best existing method is also presented. Our results demonstrate the robustness and the effectiveness of our methods for solving the duality problem. In addition, we have developed a new dataset for estimating 3D orientation of the circular feature (AlZoubi, 2014).

2 RELATED WORK

The 3D location estimation problem has been addressed in the literature. Several methods are based on point feature (Fischler and Bolles, 1981; Linnainmaa

AlZoubi A., K. Kleinhappel T., W. Pike T., Al-Diri B. and Dickinson P..
Solving Orientation Duality for 3D Circular Features using Monocular Vision.
DOI: 10.5220/0005262402130219
In *Proceedings of the 10th International Conference on Computer Vision Theory and Applications* (VISAPP-2015), pages 213-219
ISBN: 978-989-758-090-1

et al., 1988), line feature (Lowe, 1984) or quadratic curve features (Safaee-Rad et al., 1992; Shiu and Ahmad, 1989). Circular feature, as a special case of quadratic curves, has been commonly used in many computer vision application areas such as tracking, 3D pose estimation and camera calibration problems. (Chen et al., 2004) proposed a camera calibration method to estimate the parameters of the camera using single image of two circles under certain assumptions. A closed form analytical geometry method for 3D localization problem for a circular feature was presented by (Safaee-Rad et al., 1992). This method has several advantages: it provides the 3D orientation and position of a circular feature using a single camera and provides a geometrical representation for the problem. However, the method yields to two solutions, of which only one corresponds to actual orientation of the object. The method constructs the 3D conic surface from the straight lines that pass through the optical centre (centre of the camera lens which represent the vertex of the cone) and intersect the circular object on its boundary. Using this approach, the general equation of the cone with respect to image frame (xyz) is defined as:

$$ax^2+by^2+cz^2+2hxy+2gxz+2fyz+ 2ux+2vy+2wz+d=0. \quad (1)$$

and the homogenous representation of this equation can thus be written as XHX^T. Where $X = \begin{bmatrix} x & y & z \end{bmatrix}^T$ and the matrix H.

$$H=\begin{bmatrix} a & h & g \\ h & b & f \\ g & f & c \end{bmatrix} \quad (2)$$

If the object plane where the circular feature locate (the intersection plane) is defined as: $lx+my+nz=0$, then, after knowing the equation of the quadric cone, the task of finding the object plane reduces to finding an intersection plane for which the intersection is a circle. This can be expressed mathematically by determining the coefficients of the intersection plane *l, m,* and *n*.

If $K_1, K_2$and K_3 are the eigenvalues of the matrix H, then, the possible solutions of the surface normal vector (*l, m, n*) of the circular feature have been derived based on the property of a circle (Safaee-Rad et al., 1992) as the following:

Case 1: if $K_2 > K_1$**,** two solutions can be derived of which only one is the correct solution.

$$n=+\sqrt{\frac{K_1-K_3}{K_2-K_3}}\ ,\ m=\pm\sqrt{\frac{K_2-K_1}{K_2-K_3}}\ ,\ l=0; \quad (3)$$

Case 2: if $K_1 > K_2$, two solutions can be derived of which only one is the correct solution.

$$n=+\sqrt{\frac{K_2-K_3}{K_1-K_3}}\ ,\ m=0\ ,l=\pm\sqrt{\frac{K_1-K_2}{K_1-K_3}}; \quad (4)$$

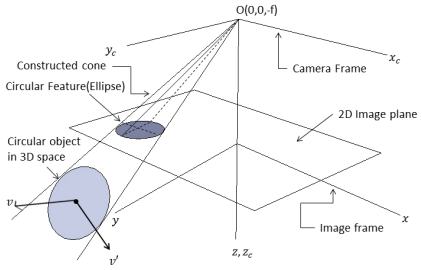

Figure 1: Schematic representation of 3D orientation estimation of circular feature and two possible orientation vectors v and v'.

Case 3: $K_1 = K_2$, this is a special case (right circular cone), indicates that the surface normal vector of the circular feature is parallel to the principle axis of the camera frame (this includes the case where the plane normal points directly to the focal point). Thus, there exists one solution where $n = 1$, $m = 0$, $l = 0$.

The method generally results in two possible orientations (true and false orientation vectors) as shown in figure 1, of which only one is correct. (Safaee-Rad et al., 1992) used a second image after a known movement of the object or the camera to resolve the duality problem. However, this solution can be applied only to static objects and requires *a priori* knowledge of the object or camera movement. In (He and Benhabib, 1998) also attempted to solve the duality problem. They proposed two methods; the first is only applicable to those features moving on a 3D line or plane with no rotational motion. The second assumes the existence of an additional reference point or line feature. However, this solution requires at least two consecutive images as well as the additional image features. It will also fail in the case that the object or the camera do not change relative position between frames. An estimation of the 3D position of the circular feature is also required.

3 OUR FRAMEWORK

We briefly describe our framework for estimating the 3D orientation of the circular feature, before proceeding to describe our methods for solving the duality problem. Our framework consists the following components:

Camera Calibration: The intrinsic camera parameters (the effective focal length f, principle point of the image plane and lens distortion factors) are estimated using (Heikkila and Silvén, 1997).

Image Enhancement: The improved adaptive background mixture model for real-time tracking with shadow detection method (KaewTraKulPong and

Bowden, 2002) is used to eliminate the image noise and detect the region of interest (RoI).

Edge Detection: The Canny edge detector method (Canny, 1986) is used to detect elliptical shapes as a set of pixel edge point data.

Lens Distortion Compensation: Radial lens distortion factors obtained in camera calibration process (Heikkila and Silvén, 1997) are used to compensate this distortion and find more accurate positions of the edge points in the RoI.

Elliptical Feature Extraction: The direct least square ellipse fitting method (Fitzgibbon et al., 1999) is applied to estimate the basic parameters of the elliptical projection of the circular object (centre, semi-major and semi-minor axes of the ellipse and theta).

3D Orientation Estimation: Using the image coordinate system with origin at the image center and *z-axis* along the cameras optical axis z_c (as shown in figure 1), the problem of estimating the circular object orientation can be reduced to finding the equation of the cone whose vertex is the center of the camera lens *(0,0,-f)* , and whose base is defined as the perspective projection of the circular feature in the image plane. Using the parameters of the circular feature, and the focal length f, the general equation of the cone (1) can be derived, and the method (Safaee-Rad et al., 1992) applied to estimate the surface normal vectors. As noted, this method results in two possible orientations as shown in figure 1.

4 OUR SOLUTIONS TO THE DUALITY PROBLEM

4.1 Reprojection of the Solutions

After parallel projection into the image plane, a 3D circle becomes an ellipse with a covariance matrix $C \in R^{2x2}$. Our first method derives the covariance matrixes for projected ellipses e and e' (in 2D space) corresponding to the vectors v and v' yielded from the method in (Safaee-Rad et al., 1992). The ellipse areas of e and e' are compared with the image ellipse in the image plane, and the "true" orientation is identified.

Let the sequence of n points describe the boundary of the circular feature p_e in 2D space, where $p_e = \{p_{ei} = (x_{ei}, y_{ei}),\ i = 1,2,3,\ \ldots n\}$ and $(x_{ei,}\ y_{ei})$ are the Cartesian coordinates of the edge points of the circular feature image.

$$C = Cov(p_e) = \begin{bmatrix} C_{xx} & C_{xy} \\ C_{yx} & C_{yy} \end{bmatrix} \tag{5}$$

The covariance matrix C is a 2 x 2, symmetric and positive definite matrix. The eigenvalues ($\lambda_1$and λ_2) and eigenvectors of the matrix C correspond to ellipse semiaxes lengths and orientation, respectively. If $\lambda_1 > \lambda_2$;then, $a = 2\sqrt{\lambda_1}$ and $b = 2\sqrt{\lambda_2}$, where a and b are semi-major and semi-minor axises, respectively.

Let the circle in 3D space which has a surface normal vector v defined as a set of points; Circle:$\{P_1, P_2 \ldots, P_n\}$ where $P_i \in R^3$ *and* $P_i = \begin{bmatrix} x_i & y_i & z_i \end{bmatrix}^T$. The Euclidean distance between the centre point of the circle (e.g. (0, 0, 0)) and any point (P_i) on the circle in 3D space can be defined as:

$$||P_i|| = \sqrt{(x_i-0)^2 + (y_i-0)^2 + (z_i-0)^2}; \tag{6}$$

where $||P_i|| \leq r$ (r is the radius of the circle), and thus the dot product of P_i and the normal to the circle v can be defined as:

$$P_i.v = \begin{bmatrix} x_i \\ y_i \\ z_i \end{bmatrix} . \begin{bmatrix} v_x \\ v_y \\ v_z \end{bmatrix} = v_x x_i + v_y y_i + v_z z_i = 0. \tag{7}$$

thus ${z_i}^2 = \frac{(v_x x_i + v_y y_i)^2}{{v_z}^2}$.

Inserting the equation of the dot product of P_i and v (7) into (6) yields to:

$$||P_i||^2 = {x_i}^2 + {y_i}^2 + \frac{(v_x x_i + v_y y_i)^2}{{v_z}^2} \tag{8}$$

Equation (8) could be written as:

$$||P_i|| = \begin{bmatrix} x_i \\ y_i \end{bmatrix}^T M \begin{bmatrix} x_i \\ y_i \end{bmatrix}. \tag{9}$$

Where $M = \begin{bmatrix} ({v_z}^2 + {v_x}^2)/\ {v_z}^2 & (\ v_x v_y)/{v_z}^2 \\ (\ v_x v_y)/{v_z}^2 & ({v_z}^2 + {v_y}^2)/\ {v_z}^2 \end{bmatrix}$.

The projected circle with normal vector v is an exact ellipse in 2D image plane and has a covariance matrix

$$C \equiv \lambda M \tag{10}$$

where $\lambda = \frac{r^2}{4}$. Equation (10) can be used to calculate the covariance matrix of the projected ellipse in 2D space for the 3D circle which has the surface normal vector v and radius r.

The proposed method for identifying the true orientation from the false one for circular feature consists of three steps:

Step 1: Calculate the covariance matrix C_o for the edge points of image ellipse e_o as defined in equation (5). The eigenvalues and eigenvectors of the matrix correspond to semiaxes lengths and orientation, respectively. The ellipse area is $A_o = ab\pi$.

Step 2: Use equation (10) to calculate the covariance matrices C and C' from the orientation vectors of the circular feature v and v' resulting from the orientation-duality. The semiaxes lengths and orientation for both

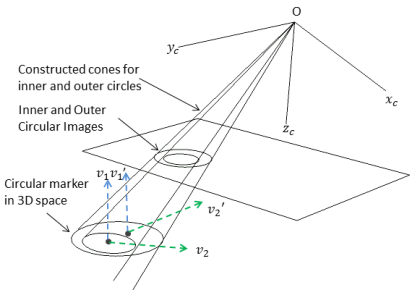

Figure 2: Schematic representation of a co-planar circle solution method for duality problem.

projected ellipses e and e' can be obtained by calculating the eigenvalues and eigenvectors of the C and C' , respectively. Finally, the areas A and A' are calculated for both e and e'.

Step 3: Check whether $A_o = A$ and $A_o \neq A'$; if true, then v is the true orientation of the circular feature.

If the orientation vector v has x and y components equal to y and x components in v' (e.g. $v = \begin{bmatrix} g_1 & g_2 & g_3 \end{bmatrix}^T$ and $v' = \begin{bmatrix} g_2 & g_1 & g_3 \end{bmatrix}^T$), then the ellipse area cannot be used to differentiate between them. However, each ellipse will be projected on different direction; therefore the eigenvectors of the covariance matrix can be used to find the true projection, and the true orientation can be identified.

If the two orientation vectors v and v' have the same components but different sign (e.g. $v = \begin{bmatrix} +g_1 & g_2 & g_3 \end{bmatrix}^T$ and $v' = \begin{bmatrix} -g_1 & g_2 & g_3 \end{bmatrix}^T$), then both vectors will result in the same covariance matrix from (10), and neither the ellipse area nor eigenvectors can be used to differentiate between them. In this case, the problem become ill-conditioned, and we cannot identify the true orientation. The case arises from the fact that the 3D circle may project into ellipse in 2D space in two different directions.

4.2 Using a Co-planar Circle

The eccentricity of the circular image that has a surface normal vector parallel to the principle axis of the camera frame is equal to zero. This value change when the circular feature moves with respect to the camera. Our co-planar circle method uses two non-coinciding circular features (inner and outer circles) to identify their mutual true orientation. Since the inner and outer circles have different centre points, the change in the eccentricity values will lead to change in the false orientation vector while the true one remains constant. The concept illustrated in figure 2. Let v_1, v_2 are the orientation vectors for inner circular image, and v_1', v_2' are the estimated orientation vectors for outer circular image. Therefore, the true orientation vector is the one that remains constant in both circular features.

Conjecture: *Co-planar circles have the same orientation with respect to the camera frame, but differences in their eccentricity will result in differences in their respective "false" orientation vectors. The inner and outer circles are co-planar, with different centre points: their common orientation vector represents their true orientation (e.g. $v_1 = v_1'$ and $v_2 \neq v_2'$).*

This method consists of two steps:

Step 1: Estimate the possible orientation vectors of the inner and outer circular features (v_1, v_2, v_1', v_2'), respectively.

Step 2: Check if $v_1 = v_1'$ and $v_2 \neq v_2'$, then v_1 is the true orientation of the circular feature.

If the diameter of the inner circle is $I_d = \frac{O_d}{2}$, with O_d being the diameter of the outer circle. Then, the method works reliably if the distance between the centre points of inner and outer circles $D \geq \frac{O_d}{5}$. The value of D has been experimentally established.

5 EXPERIMENTS

Three experiments were performed to validate the proposed methods and oveall system of estimating the 3D orientation of the circular feature: (1) The first experiment validates our first (reprojection) method for resolving the duality problem and identify the true orientation. Two groups of circle images were captured with known orientations. Each group contains five circular features with the same orientation, but different positions. Then, our reprojection method used to identify the true orientation vector for each circular feature. (2) The second experiment validates our second (coplanar circle) method for resolving the duality problem. Two groups of circular markers with inner and outer circles were used to identify the true orientations. A comparisons between our methods with best state-of-art method are presented. (3) The third experiment evaluates the accuracy of our framework for estimating the 3D orientation of the circular feature.

5.1 Setup

The experiment setup utilized the following hardware imaging components for both experiments; Canon PowerShot SX200 IS with resolution 4000x3000pixels and focal length: 5-60mm f/3.4-5.3. Adjustable Angle Mounting Plate (API180) which provides a full 180° of movement with 18arcmin precision to holds the circular features (see

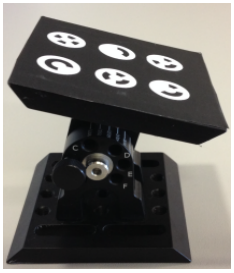

Figure 3: Circular images located on API180.

figure 3); and a 30 cm x 20 cm calibration board used for camera calibration process. Intel Core i5-2450M laptop, CPU@2.50GHz used to run the experiments.

5.2 Dataset

We have developed a new dataset for estimating 3D orientation of the circular feature. The dataset includes two subsets: the first contain images for 136 circular objects with different diameters (0.7, 1.5 and 2 cm), and different positions and orientations with respect to the camera. The second subset contains 50 images for circular markers with inner and outer circles with different positions and orientations with respect to the camera. The two subsets used to compare our methods (reprojection and coplanar circle) against current state-of-art methods. The dataset with the setup description are available in (AlZoubi, 2014).

5.3 Verification of Reprojection Method

The method was verified by experiments using circular objects locates at distance 60cm from the camera. Two groups of image circles with different orientations were acquired using the Canon camera. The diameter of the circular objects in group 1 was 0.7 cm and the diameter of the objects in groups 2 was 1.5 cm. Each group has five circular features located on API180 at distances (20, 30, 40, 50 and 60cm) from the centre of the image plane. Using API180, the orientation vector and orientation angles of the circles' planes were then estimated. These are referred to as reference orientation vector and reference angle (which represent the ground truth). The computational procedures of our framework were applied to estimate the orientation vectors v and v' for each circular image. Following steps 1 through 3 in 4.1; the projected ellipses e and e' from the vectors v and v' , are computed and compared with the image ellipse e_o in the image plane. The relative changes R_1 and R_2 in the ellipses areas A and A' comparing with A_o were calculated for the five circular images in each group (where $R_1 = \frac{|A-A_o|}{A_o}$ and $R_2 = \frac{|A'-A_o|}{A_o}$). The results of

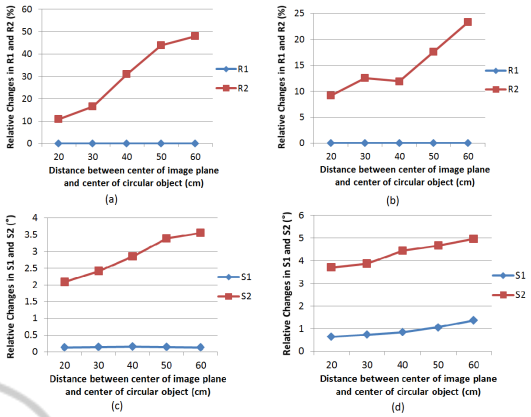

Figure 4: (a) changes in R_1 and R_2 in group 1 of circular images with rotation 75°, 90°,15° around x, y, and z axes, respectively; (b) changes in R_1 and R_2 in group 2 of circular images with rotation 60°, 90°,30° around x, y, and z axes, respectively; (c) changes in S_1 and S_2 in group 3 of circular images with rotation 75°, 90°,15° around x, y, and z axes, respectively; (d) changes in S_1 and S_2 in group 4 of circular images with rotation 60°, 90°,30° around x, y, and z axes, respectively.

the two groups are shown in figures 4(a) and (b). Figure 4(a) shows the results for the five circular features in group 1, these circular features were located at different positions with same orientation (75°, 90°,15° around x, y, and z axes, respectively). The relative changes between A and A_o (which represent R_1) are very small and varies between the values 0.007% to 0.05%, while the relative changes between A' and A_o (which represent R_2) are varies between the values 9.5% to 23.8%. Thus, e is clearly the true projection of ellipse in 2D space and match the image ellipse e_o in the image plane. As can be noted from figures 4(a) and (b), R_1 in the two groups are almost equal to zero, while the change in R_2 varies significantly. Thus, e is the true projection of ellipse in 2D space, and therefore, v is the true orientation for the circular feature and v' is the false one in this case.

5.4 Verification of Co-planar Circle Method

The co-planar circle method for solving orientation-duality problem was verified by experiments using a circular marker which consist inner and outer circles with different centre points. The inner and outer circles have 1 cm and 2 cm diameters, respectively. The distance between the centre points of the inner and outer circles was 0.4 cm. Two groups of circular markers with different orientations were acquired at distance 60 cm from the camera. Each group contains five markers located on the API180 and have

Table 1: Estimated orientation angles of the surface normal of a set of circular images.

Angles	$\alpha(^\circ)$	$\beta(^\circ)$	$\gamma(^\circ)$
Reference Angle	75	90	15
Circle 1	76.16	88.57	13.91
Circle 2	76.44	89.55	12.99
Circle 3	76.17	88.17	12.97
Circle 4	76.77	89.75	13.42
Circle 5	74.93	89.89	16.26
Circle 6	74.78	89.94	15.54
Average	75.87	89.31	14.18
Average Deviation	**0.87**	**0.69**	**0.82**

the same orientation. The markers were located at distances (20, 30, 40, 50 and 60 cm) from the centre of the image plane. The computational procedures of our framework were applied to estimate accurately the possible orientation vectors for inner and outer circular features (v_1, v_2, v_1' and v_2'), respectively. The API180 was used to define the reference orientation vector and reference angles (which represent the ground truth). Following steps 1 and 2 in 4.2, the relative changes S_1 and S_2 in the parameters v_1, v_2, v_1' and v_2' were calculated for the five circular markers in each group (where $S_1 = Angle(v_1, v_1')$ and $S_2 = Angle(v_2, v_2')$). Since the inner and outer circular feature are co-planar; the mutual orientation vector between both of them is the true one, and therefore, the angle between the true orientation vectors in both circles must be equal to zero. The results for the two groups are shown in figures 4(c) and (d). Figure 4(c) shows the results for the five circular markers in group 3, these markers were located at different positions with same orientation (75°, 90°,15° around x, y, and z axes, respectively). The angles between v_1 and v_1' (which represent S_1) are:0.13°, 0.14°, 0.15°. 0.14°, and 0.13° for the five circular markers, respectively. The angles between v_2 and v_2' (which represent S_2) are: 2.09°,2.41°,2.85°,3.4°, and 3.55° for the five circular markers, respectively. The values for S_1 are very small, while the values in S_2 are higher. Thus, S_1 is clearly the true solution, and therefore v_1 is the true orientation vector. Similarly, group 4, as shown in figure 4(d), has values of S_1 are almost equal to zero, while the changes in S_2 varies significantly.

Comparison with the Existing Method. The dataset described in section 5.2 was used to compare the performance of our methods (reprojection and co-planar circle) against the co-planar point method proposed in (He and Benhabib, 1998). The dataset is challenging due to the different objects diameters, the objects loacted in different positions and orientations with respect to the camera, and the existence of noise. Using API180, the orientation angles of the circles were estimated and used as a ground truth. The three methods were applied to the whole dataset. The method (He and Benhabib, 1998) fails in 54% of cases due to (1) identify the false orientation as true in 5% of the dataset, (2) the method was not able to differentiate between the co-planar point and the noise points in 19%, and (3) the method fails in 30% of the dataset because the objects do not move between consecutive frames. In contrast, the reprojection method and the co-planar circle method were able to identify the true orientation of the circular objects in all cases, even with the existence of noise or in the case where the object stays in same location for two or more consecutive frames.

5.5 Evaluating Orientation Accuracy

The accuracy of our framework for estimating the orientation of circular objects was tested on a group of six co-planar circular images. The diameter of each circular object was 0.7 cm and they were located at distance 60 cm from the camera. Figure 3 shows a sample of an image circles (tags) located on API180. The computation procedures of our framework (including the reprojection method) were applied to estimate the 3D orientation for each circular feature. Using API180, the orientation angles of the circles plane is then estimated. These are referred to as the "Reference Angle" in Table 1, which shows the results of the estimated orientation for each circular feature. The six circles have the same orientation, since they are co-planar. We have defined the average deviation of the orientation as the absolute value of the difference between the reference angle and the average angle, measured as (0.87°, 0.69°, 0.82°) rotation around *x, y* and *z axes*, respectively. Note: α, β, and γ are the angles that the surface normal of a circle makes with the *x, y,* and *z axes* of the camera frame.

6 CONCLUSION

Two novel methods for solving the orientation-duality problem have been proposed. The first compares features from the 2D projects of both solutions with the ellipse image in the image plane. This method solves, and for the first time, the orientation duality problem using a single 2D image without requiring additional geometrical and texture features, nor an estimate of the 3D position. The method has been tested on circular objects with different orientations, positions and different objects sizes. The experimental results showed that the method is robust and perform better than existing methods. One ill-conditioned case has

been identified; however, it can be detected and eliminated during run-time by acquiring another image of the moving object. The second method relies on using two non-coinciding co-planar circles, to identify their mutual true orientation. This method does not require multiple images nor a position estimate. The method could be very useful for recognition of moving objects with circular markers as target to be tracked. The method has been tested on circular objects with different orientations, positions and object sizes. The experimental results showed that the method can identify the true orientation effectively and perform better than existing methods. Our framework showed only a small error for estimating the orientation of circular feature (less than 1°). The proposed methods are effective and solve the orientation-duality problem for both static and object in motion, and it can be used to identify the actual orientation of the circular objects in real applications. Our system could be applicable for tracking pre-marked animals (such as fish), and it has applications in machine vision (e.g. tracking mobile robot using circular marker), and autonomous takeoff and landing of a Micro Aerial Vehicle. It could also used to estimate eye gaze using a single 2D image.

REFERENCES

AlZoubi, A. (2014). 3dfishtrack: www.3dfishtrack.com.

Canny, J. (1986). A computational approach to edge detection. *Pattern Analysis and Machine Intelligence, IEEE Transactions on*, (6):679–698.

Chen, Q., Wu, H., and Wada, T. (2004). Camera calibration with two arbitrary coplanar circles. In *Computer Vision-ECCV 2004*, pages 521–532. Springer.

Fischler, M. A. and Bolles, R. C. (1981). Random sample consensus: a paradigm for model fitting with applications to image analysis and automated cartography. *Communications of the ACM*, 24(6):381–395.

Fitzgibbon, A., Pilu, M., and Fisher, R. B. (1999). Direct least square fitting of ellipses. *Pattern Analysis and Machine Intelligence, IEEE Transactions on*, 21(5):476–480.

He, D. and Benhabib, B. (1998). Solving the orientation-duality problem for a circular feature in motion. *Systems, Man and Cybernetics, Part A: Systems and Humans, IEEE Transactions on*, 28(4):506–515.

Heikkila, J. and Silvén, O. (1997). A four-step camera calibration procedure with implicit image correction. In *Computer Vision and Pattern Recognition, 1997. Proceedings., 1997 IEEE Computer Society Conference on*, pages 1106–1112. IEEE.

KaewTraKulPong, P. and Bowden, R. (2002). An improved adaptive background mixture model for real-time tracking with shadow detection. In *Video-Based Surveillance Systems*, pages 135–144. Springer.

Linnainmaa, S., Harwood, D., and Davis, L. S. (1988). Pose determination of a three-dimensional object using triangle pairs. *Pattern Analysis and Machine Intelligence, IEEE Transactions on*, 10(5):634–647.

Lowe, D. G. (1984). Perceptual organization and visual recognition. Technical report, DTIC Document.

Safaee-Rad, R., Tchoukanov, I., Smith, K. C., and Benhabib, B. (1992). Three-dimensional location estimation of circular features for machine vision. *Robotics and Automation, IEEE Transactions on*, 8(5):624–640.

Shiu, Y. C. and Ahmad, S. (1989). 3d location of circular and spherical features by monocular model-based vision. In *Systems, Man and Cybernetics, 1989. Conference Proceedings., IEEE International Conference on*, pages 576–581. IEEE.

Wang, J., Sung, E., and Venkateswarlu, R. (2003). Eye gaze estimation from a single image of one eye. In *Computer Vision, 2003. Proceedings. Ninth IEEE International Conference on*, pages 136–143. IEEE.

Xu, W., Xue, Q., Liu, H., Du, X., and Liang, B. (2012). A pose measurement method of a non-cooperative geo spacecraft based on stereo vision. In *Control Automation Robotics & Vision (ICARCV), 2012 12th International Conference on*, pages 966–971. IEEE.

Yoon, Y., DeSouza, G. N., and Kak, A. C. (2003). Real-time tracking and pose estimation for industrial objects using geometric features. In *Robotics and Automation, 2003. Proceedings. ICRA'03. IEEE International Conference on*, volume 3, pages 3473–3478. IEEE.

Young, R. A. (1987). Locating industrial parts with subpixel accuracies. In *Cambridge Symposium_Intelligent Robotics Systems*, pages 2–9. International Society for Optics and Photonics.